Analysis of the Potential for Site Ventilation to Improve Overall Efficiency of Utility-Scale Solar Farms

Henry J. Williams, Yuming Sun, Khaled Hashad, K. Max Zhang

Sibley School of Mechanical and Aerospace Engineering, Cornell University, Ithaca, NY 14850, United States

ABSTRACT

Utility scale solar farms are being rapidly developed to reduce carbon footprint and to help meet ambitious energy goals set by state and federal governments. Using computational fluid dynamics (CFD), we are developing comprehensive design tools to investigate the microclimate of a solar farm. In this study, we define the term "ventilation" to qualitatively assess wind flow through a solar farm and measure its effect on solar module efficiency. We model a solar farm and compare the simulation results to a modified site design with improved ventilation. This investigation provides a basis for further studies on design and predictive models of solar farms, and it makes an argument for combining agriculture and photovoltaics through agrivoltaics.

Keywords: CFD, solar PV, solar module efficiency

NONMENCLATURE

Abbreviations	
CFD	Computational Fluid Dynamics
PV	Photovoltaic
STC	Standard Test Conditions
RNG	Renormalized-group
RTE	Radiative Transfer Equation

1.   INTRODUCTION

Large-scale solar energy development is critical to mitigating climate change impacts. A recent Department of Energy study shows the need to install 30-60 GW of solar photovoltaics (PV) each year between 2021 and 2030 in the US to achieve 95% grid decarbonization by 2035 [1]. The design of large-scale solar farms deserves rigorous testing and research as they are being rapidly developed to meet these energy goals.

Yu and Fthenakis investigated a 1 MW section of a solar farm to explore the heat island effect in the local microclimate [2]. Stanislawski et al. explored the relationship between solar site layout and heat transfer coefficient using Large-Eddy Simulations (LES) [3]. We aim to show that a comprehensive thermal-fluidic model evaluated against real data can be used to propose key design changes to improve solar module efficiency.

Solar modules experience losses in efficiency at temperatures higher than the Standard Test Condition (STC) of 25°C [3]. Even in the cold-climate solar farm analyzed here, results show that module temperatures approach 55°C. Traditional solar farms experience efficiency loss by impeding the convective cooling effect of wind flow with tightly-packed arrays. Thus, we posit that adding gaps between PV arrays can increase solar farm efficiency through improved ventilation. (**Fig. 1**).

In this study, we develop a transient thermal-fluidic model to explore a section of a solar farm in Ontario, Canada, using weather station data for inlet conditions. We evaluate the model against real data and propose a new design, allowing us to explore the effect of site ventilation on the overall efficiency of a solar farm.
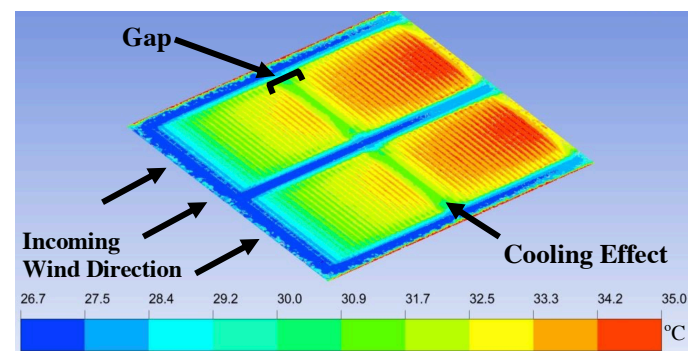

Fig. 1. Convective cooling in a 1 MW section of a solar farm

2.   METHODS

2.1 Basic Thermal Model

Solar module surface temperature is sensitive to solar radiation, convective heat transfer, and radiative heat loss to the surrounding environment (**Fig. 2**).
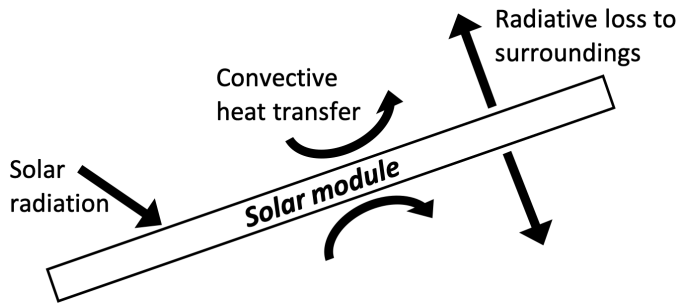
Fig. 2. Heat transfer on a solar module (cross sectional view)

2.2 CFD Set-up

We used Ansys Fluent to develop our CFD model. For turbulent flow, we selected the renormalized-group (RNG) k-ε turbulence scheme, as it includes the effect of swirl on turbulence and provides an analytical formula for turbulent Prandtl numbers [5]. Buoyancy effects were enabled to capture turbulence generated in a gravity field and temperature gradient [5].

Using the P-1 radiation model, the Radiative Transfer Equation (RTE) is treated as a diffusion equation and includes scattering effects [5]. We input geographic location, cardinal orientation, and chronological day to the Solar Load feature to capture the position of the sun. The solar farm location in this investigation is 82.34°W, 42.94°N, and weather station data was taken on July 1, 2011. Global solar irradiation was modeled as a time-dependent polynomial expression which estimates real solar radiation data obtained from the solar farm (**Fig. 3)**:

$$I = 1.0 * 10^{-15}t^4 - 1.9 * 10^{-10}t^3 \quad (1)$$
$$+ 1.1 * 10^{-5}t^2 - 2.4 * 10^{-1}t + 1.7 * 10^3$$

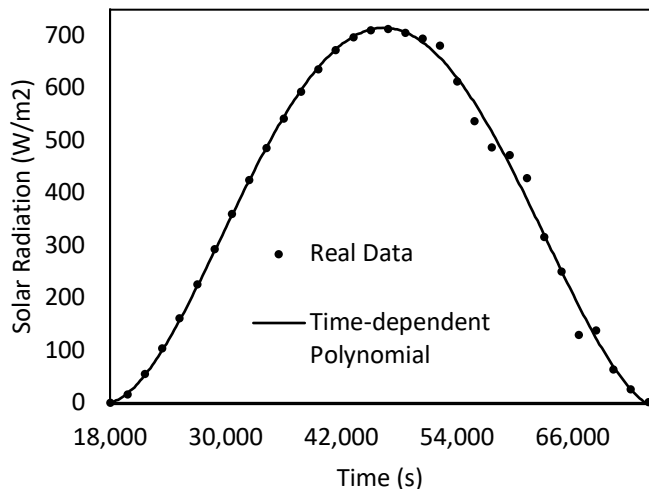where I is direct solar irradiation (Wm^{-2}) and the variable t is time (s).

Fig. 3. Time-dependent polynomial based on radiation data

Solar radiation is modeled between 18,000s and 75,600s from midnight, or 5:00 am to 9:00 pm. Before 5:00 am and after 9:00 pm, solar radiation is effectively zero. Thus, the model is initiated at 12:00 am with zero radiation until 5:00 am, at which point radiation is determined by Equation (1). After 9:00 pm, radiation is considered zero again.

V. Fthenakis provided field data [2]. Wind speed and ambient temperature were read into model in 30-minute increments for inlet and outlet conditions. Radiation boundary conditions were enabled for PV modules and ground, with corresponding material properties in **Table 1** [6], [7]. The solver used the pressure-based SIMPLE algorithm with second order discretization schemes.

Table 1. Material properties for PV modules and ground

Material	PV Module [6]	Ground [7]
Density (kg/m³)	2330	1000
Specific Heat (j/kg-K)	677	1000
Thermal Conductivity (W/m-K)	148	0.35

2.3 Physical Model

A 3-D geometry was constructed with four fields separated by 8.0m gaps (**Fig. 4**). Each module measures 0.60m*1.2m. Each array contains 180 modules, mounted 25° from the horizon and placed every 4.0m [2].
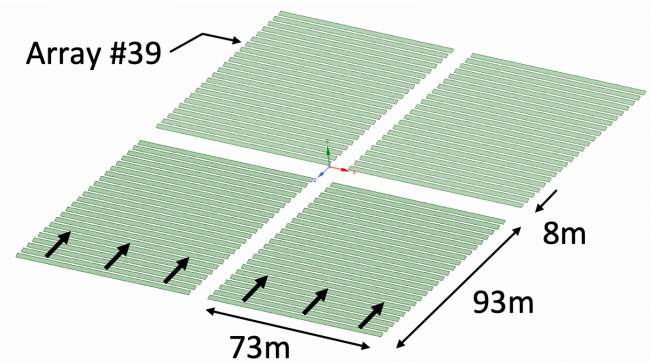

Fig. 4. Geometry of a 1 MW section of a solar farm, with wind direction indicated by arrows

The original geometry, *Design 1*, was left unchanged from the site layout in Ontario, with 46 arrays in each symmetric half as shown in **Fig. 5** (a). The modified geometry, *Design 2*, was created by removing a single array in the 39th position from the inlet as shown in **Fig. 5** (b). This modification was made to demonstrate improved ventilation with the added gap due to the convective cooling effect of wind across the space between solar arrays.
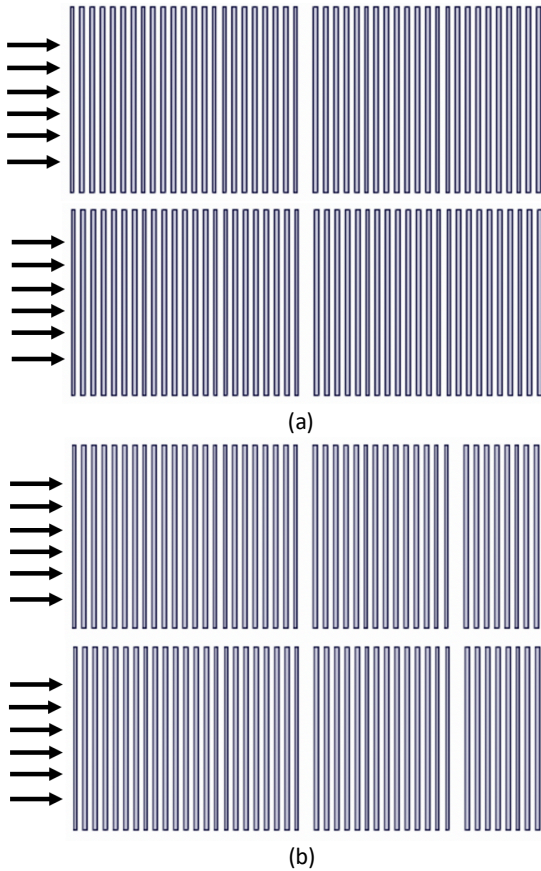
　　　　　　　　　　　　　　　　Copyright © 2021 ICAE

(a)

(b)

Fig. 5. (a) Top-view of Design 1 and (b) Design 2

Fig. 6 (a) shows the mesh section view from the side profile of Design 1 (640,529 elements), while **Fig. 6** (b) shows the mesh section view from the side profile of Design 2 (634,383 elements). A local element size of 1.0m was used at the surface of the PV arrays, and the growth rate was set to 1.2 so the mesh could expand within the domain, which extended 40m to the top and sides, 60m at outlet, and 0.50m to the ground.
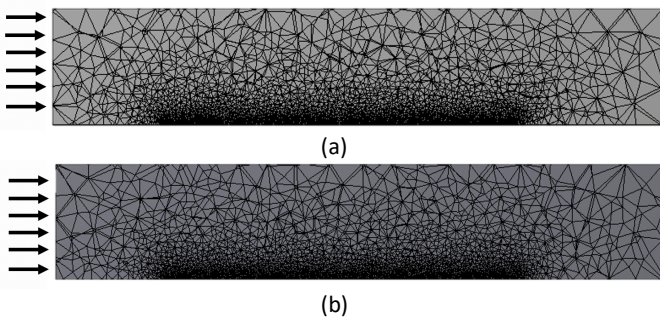

(a)

(b)

Fig 6. (a) Mesh section view of Design 1 and (b) Design 2

3.   THEORY AND CALCULATION

3.1 Properties at STC

Convective cooling from wind decreases PV module surface temperature, and therefore increases overall efficiency and power production. The solar farm in this investigation uses Module FS275, a solar cell module developed by First Solar [8]. **Table 2** shows module specifications at STC, where P_{ref} is nominal power, A_{ref}, is nominal size, and β_{ref} is the temperature coefficient [8].

Table 2. Module FS275 nominal properties

Nominal power (P_{ref})	75 W
Nominal area (A_{ref})	0.72 m^2
Temperature coefficient (β_{ref})	0.25%/^{o}C

3.2 Power and Efficiency Calculation

Solar module surface temperature was measured every 30 minutes for each array. Results show that 2:00 pm yields the highest surface temperatures.

The total nominal power, $P_{tot,ref}$, of the solar site can be calculated as [7]:

$$P_{tot,ref} = P_{ref} N_f N_m N_a \qquad (2)$$

where N_f is number of fields, N_m is number of modules, and N_a is number of arrays.

PV module efficiency, η_{ref}, at STC is given by [9]:

$$\eta_{ref} = \frac{P_{ref}}{A_{ref} G_{ref}} \qquad (3)$$

where G_{ref} is incident radiation at STC (1000 Wm^{-2}). Module FS275 is a thin-film type and therefore has a relatively low maximum efficiency of 10.417% using equation (3) [8].

PV cell efficiency, η_c, at a selected operating temperature is given by [10]:

$$\eta_c = \eta_{ref}[1 - \beta_{ref}(T_c - T_{ref})] \qquad (4)$$

where T_c is the cell module operating temperature and T_{ref} is the temperature at STC (25°C).

The actual power produced for a given number of arrays is given by [9]:

$$P = \eta_c N_a A I \qquad (5)$$

where A is area and I is radiation (Equation (1)).

4.   RESULTS

4.1 CFD Model Validation

The CFD model was evaluated using real module surface temperature from the Ontario site on July 1,

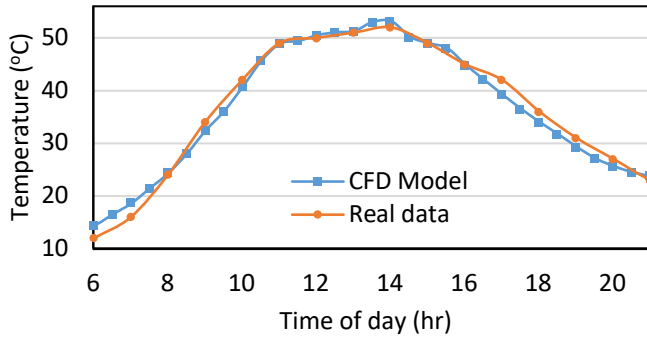2011, corresponding to inlet conditions from weather station data on the same day (**Fig. 7**).

Fig. 7. PV module surface temperature evaluation

4.2 Module Surface Temperature at 2:00pm

We examined the entire solar farm at 2:00 pm, when the PV module surface temperatures reached a peak. **Fig. 8** shows PV module surface temperature for all arrays, noting the first gap present in both designs, and the second gap in Design 2.
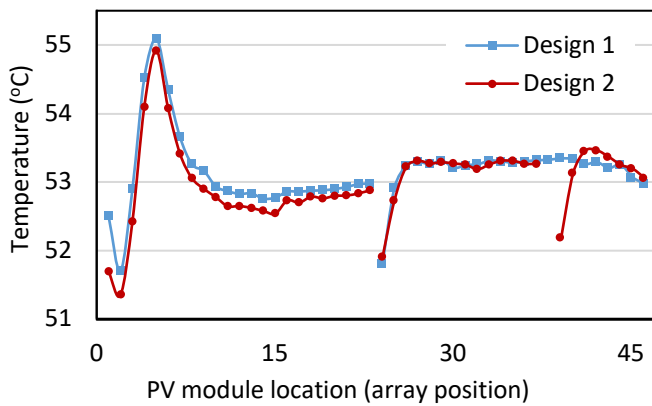

Fig. 8. PV module surface temperature distribution at 2:00 pm

Table 3 shows total nominal power, given by Equation (2), compared to actual power, given by Equation (5), produced at 2:00 pm. Total efficiency is reported as a ratio of actual to nominal power.

Table 3. Power data at 2:00 pm for Design 1 and 2

Design #	1	2
Nominal power, $P_{tot,ref}$ (MW)	1.24	1.21
Actual power, P (MW)	0.826	0.808
Total efficiency, $100P/P_{tot,ref}$	66.6%	66.7%

4.3 Module Surface Temperature at Array #39

Array #39, noted in **Fig 4**, is the array most affected by inserting the gap in Design 2. We examined the array during peak sunlight hours, 11:00 am – 3:00 pm, when the solar farm experiences the most radiative heat flux.

Fig. 9 shows a comparison between the PV module temperature with corresponding efficiency, given by Equation (4), for array #39.
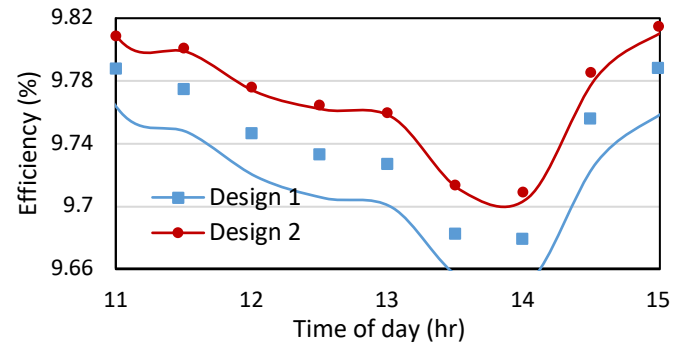

Fig. 9. PV efficiency for array #39 during peak sunlight hours

Table 4 shows actual power produced by Design 1 and 2 during peak sunlight hours for array #39.

Table 4. Actual power during peak sunlight hours (array #39)

	Actual power, P (MW)	
Time of day	Design 1	Design 2
11:00 am	0.809	0.810
12:00 pm	0.882	0.885
1:00 pm	0.899	0.902
2:00 pm	0.872	0.875
3:00 pm	0.778	0.780

5. DISCUSSION

5.1 Effect of Site Ventilation

Fig. 8 shows that Design 2 is effective in lowering the module surface temperature of array #39 by adding a second gap. **Table 3** shows that Design 2 ultimately produces 18 kW less power than Design 1, as removing an entire array lowers the overall surface area. However, the design change yields 0.1% efficiency improvement for the entire solar farm (**Table 3**).

Focusing on array #39, it is clear that the lowered temperature directly results in a higher efficiency (**Fig. 9**). During peak daylight hours, Design 2 shows an average 2 kW increase in actual power for the single array (**Table 4**). Applied over an entire solar farm, this would make a large impact on total power production.

These results are based on a cold-climate solar farm using real wind speeds varying between 1-2 m/s. With higher wind speeds and ambient temperatures, Design 2 would see an increased margin in efficiency and power production.

5.2 Implications for Agrivoltaics

Agrivoltaic farms combine conventional agriculture and solar PV, the value of which yields a 30% increase in economic value relative to conventional agriculture [11]. Agrivoltaic sites employ large interrow gaps to increase incident radiation on crops. The results of this study demonstrate that the spacing in agrivoltaic farms make them more efficient than traditional solar farms.

6. CONCLUSION

A comprehensive understanding of convective cooling on a solar farm due to wind is vital to designing utility-scale solar power plants. In this study, we defined "ventilation" as a qualitative assessment of wind flow over a solar farm. Improved ventilation increases convective cooling on PV module surfaces, resulting in efficiency and power gains. Using a model validated by real data, we have shown that incorporating gaps in solar farms improves ventilation and provides an argument for agrivoltaic dual-use site design.

ACKNOWLEDGEMENTS

REFERENCES

[1] US Dept. of Energy. *Solar futures study.* 2021.
[2] Yuanhao Yu, Fthenakis, V. *Analysis of the potential for a heat island effect in large solar farms*. IEEE. 2013; 3362-3366.
[3] Stanislawski, B., et al. Potential of module arrangements to enhance convective cooling in solar photovoltaic arrays. *International Journal of Renewable and Sustainable Energy.* 2020; 157: 851-858.
[4] Perraki, V., Tsolkas, G. Temperature dependence on the photovoltaic properties of selected thin-film modules. *International Journal of Renewable and Sustainable Energy.* 2013; 2: 140-146.
[5] Theory Guide, *Ansys Fluent Manual 15*
[6] Kant, K., et al. Heat transfer studies of photovoltaic panel coupled with phase change material. *Solar Energy*. 2016; 140: 151–161.
[7] Armstrong, S., Hurley, W.G. A thermal model for photovoltaic panels under varying atmospheric conditions. *Applied Thermal Engineering*. 2010; 20(11-12): 1488-1495.
[8] First solar FS series 2 PV module specification sheet, https://www.firstsolar.com/-/media/First-Solar/Technical-Documents/Series-2-Datasheets/Series-2-Module-Datasheet-NA.ashx?la=en.
[9] Beckman. Solar engineering of thermal processes, 4th ed. Hoboken, N.J.: John Wiley & Sons; 2013.
[10] Van Donk, S., Tollner, E. W. Apparent thermal conductivity of mulch materials exposed to forced convection. *American Society of Agricultural Engineers*. 2000; 43(5): 1117-1127.
[11] Dinesh, Harshavardhan; Pearce, Joshua M. The potential of agrivoltaic systems. *Renewable and Sustainable Energy Reviews*. 2015; 54: 299–308.